# INVESTIGATION OF FLOW CHARACTERISTICS IN HEAT EXCHANGER TUBE BUNDLES COMPOSED OF WAVY AND CIRCULAR CYLINDERS

K. Lam, Y. F. Lin, T. Cai, Y. Liu

*Department of Mechanical Engineering, The Hong Kong Polytechnic University, Kowloon, Hong Kong*

L. Zou

*School of Mechanical and Electronic Engineering, Wuhan University of Technology, Wuhan, P.R.China*

## ABSTRACT

*The present investigation aims at controlling the FIV by using the combinations of wavy and circular tube bundles. Three types of tube bundles are studied with the first row of tubes replaced by different wavy cylinders and compared with circular cylinders only. Due to the effect of wavy tubes introduced at the first row, the wake patterns of the second row tubes become well organized and the vortices shedding there shift to further downstream positions. As a result, the fluctuating forces of the tube bundles are significantly weakened.*

## 1. INTRODUCTION

Tube bundles are widely employed in cross-flow heat exchangers. However, flow-induced vibrations (FIV) of heat exchanger tube bundles often result in serious structural failure. Over the past years, numerous experimental investigations have been carried out to study the mechanism of FIV in different configurations of tube bundles, such as Price et al. (1995), Rottmann and Popp (2003) and Paul et al. (2007). Because of the complicated flow characteristics in the heat exchanger tube bundles, the vortex structures can not be clearly observed and some valuable information can not be obtained by experimental techniques alone. It is anticipated that numerical simulations would be able to capture the instantaneous three-dimensional vortex structures and other valuable information, such as drag, lift, pressure, velocity and Reynolds stress, etc. Successful numerical investigations of flow around tube bundles had been carried out by Barsamina and Hassan (1997), Kevlahan and Wadsley (2005) and Schneider and Farge (2005). Moreover, based on the idea of modifying the tube shapes, Horvat et al. (2006) investigated the heat transfer conditions of the tube bundles with different tube shapes.

In our previously investigations, we found that a cylinder with wavy surface can well weaken even suppress the FIV compared with a circular cylinder at the same Reynolds numbers (Lam et al. 2004a, b). The optimal spanwise wavelengths ($\lambda/D_m \approx 2$ and 6) for drag reduction and vibration suppression were found (Lam and Lin 2007, 2008). An extension of investigation on a row of wavy cylinders, Lam et al. (2007) showed that the wavy cylinders give rise to a more stable flow pattern with less fluctuation and longer wake vortex closure length compared with a row of circular cylinder.

Based on these results, the present investigation aims at controlling FIV of the heat exchanger tube bundles by using the combinations of wavy and circular tube bundles. It is hoped that by replacing the certain circular cylinders with wavy cylinders in heat exchangers, the effects of flow-induced vibration could be minimized. When the spacing ratio between the cylinders is small, the effect of flow interference is significant. Therefore, it is necessary to study identify the advantages of replacing circular cylinders with wavy cylinders. The finite volume method (FVM) is employed to simulation the flow pass the wavy and circular tube bundles. For the turbulent flow, the large eddy simulation (LES) is adopted. Also, experimental measurements using the Laser Doppler Anemometer (LDA) technique is carried out to supplement the study. The time-average velocity distributions of flow field are obtained. Both the laminar flow and turbulent flow conditions are examined.

## 2. TUBE BUNDLE MODELS

Figures 1a, b, & c show the three types of tube bundles being studied. For (b) and (c), the first row of tubes is replaced by different wavy cylinders compared with that of purely circular cylinders (a). The tubes are in staggered arrangements. There are two kinds of wavelength ratios being used ($\lambda/D_m$=1.5 or 6) with a fixed wave amplitude $a/D_m$=0.15 (refer to table 1). In the first row, the wavy tubes are arranged out-of-phase according to our previous study (Lam et al. 2007).

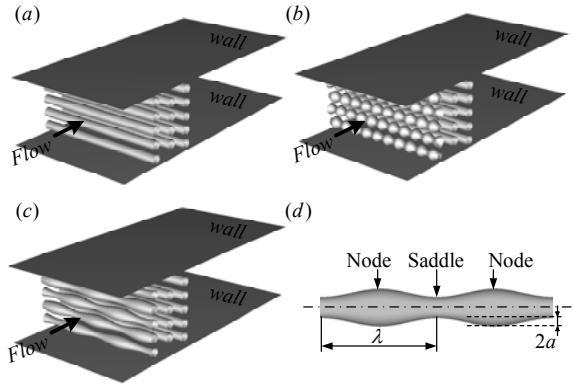


Figure 1: *Three types of tube bundles ; (a) first row of tubes arranged with circular cylinders; (b) first row of tubes arranged with wavy cylinders ($\lambda/D_m$=1.5, $a/D_m$=0.15); (c) first row of tubes arranged with wavy cylinders ($\lambda/D_m$=6, $a/D_m$=0.15); (d) The geometry of wavy cylinder models.*

The geometry of the wavy cylinder is described by the equation, $D_z = D_m + 2a\cos(2\pi z/\lambda)$ (see figure 1(d)). Here, $D_z$ denotes the local diameter of the wavy cylinder and $D_m = (D_{min} + D_{max})/2$ is the mean diameter. $D_{min}$ is the minimum diameter along the spanwise direction, while $D_{max}$ is the maximum diameter of the wavy cylinder. The amplitude of the curve surface is denoted by '$a$', and '$\lambda$' is the wavelength along the spanwise direction. The axial locations of the maximum local diameter are referred to as "nodes", while the axial locations of the minimum diameter are called "saddles".

| First row of tubes | $\lambda/D_m$ | $a/D_m$ |
|---|---|---|
| Circular cylinder (CY) | - | - |
| Wavy cylinder-A (WY-A) | 1.5 | 0.15 |
| Wavy cylinder-B (WY-B) | 6.0 | 0.15 |

*Table 1: Parameters of the wavy tubes.*

### 2.1 Experimental setup

The present LDA measurements were carried out in a closed-loop water tunnel with a rectangular working section, including the $x$, $y$ and $z$ velocity measurements. The test-section is made of Perspex. An overview of the experimental system with the setup arrangements are shown in figures 1 and 2. The staggered tubes were assigned by numbers 1-5 for the first row from the upstream position. The numbers 6-9 and 10-14 were assigned at the middle and downstream tubes, respectively. The spacing ratio of the tubes in each tube rows are fixed at $1.5D_m$, while the spacing ratio between the tubes rows are $2.5D_m$. The tubes height for the present experimental measurements is equal to $15D_m$.

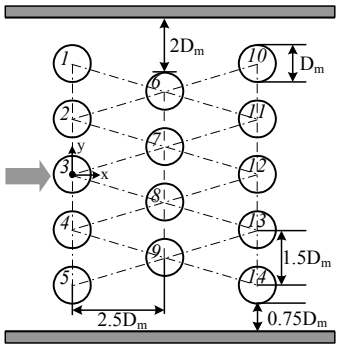


Figure 2: *The sketch of tube bundle arrangement.*

In order to obtain the mean and fluctuating velocity data, a two-colour fiber-optic LDA was employed. It was operated in the backscatter mode and with a frequency shift. The signals from the photomultipliers were analyzed using a correlation-technique LDA signal processor (DANTEC model 58N40 two-component LDA with enhanced FVA signal processor). The LDA system comes with the software for data processing and analysis. Therefore, the profiles of the mean velocity, fluctuating velocity and the shear stresses along the $x$-, $y$- and $z$-direction could be achieved simultaneously and automatically by sampling the data following the $x$, $y$ and $z$ coordinate sequence.

### 2.2 Numerical method

Both the laminar and turbulent models are performed in the present study. For the turbulent flow, by using the LES turbulence model, the large scale eddies are solved directly by the filtered Navier-Stokes equations, and the small eddies are modeled using a subgrid scale (SGS) model. The governing equations employed for LES are

$$\frac{\partial \overline{u}_i}{\partial x_i} = 0. \quad (1)$$

$$\frac{\partial \overline{u}_i}{\partial t} + \frac{\partial \overline{u}_i \overline{u}_j}{\partial x_j} = -\frac{1}{\rho}\frac{\partial \overline{p}}{\partial x_i} + \nu \frac{\partial^2 \overline{u}_i}{\partial x_j x_j} - \frac{\partial \tau_{ij}}{\partial x_j}. \quad (2)$$

where $\overline{u}_i$ are the filtered velocity components along the Cartesian coordinates $x_i$, $\overline{p}$ is the pressure, $\rho$ is the fluid density, $\nu$ is the kinematic viscosity of the fluid and $\tau_{ij}$ is the subgrid scale stress, given as

$$\tau_{ij} = \overline{u_i u_j} - \overline{u}_i \overline{u}_j. \quad (3)$$

The detailed descriptions of the presents LES

method can be found in Lam and Lin (2008). Furthermore, the finite-volume method (FVM) applied on unstructured grids is employed to solve the unsteady incompressible Navier-Stokes equations. A second-order central differencing scheme is used for momentum discretization while a second-order implicit scheme is employed to advance the equations in time. The pressure implicit method with splitting of operators (PISO) algorithm is used to deal with the pressure-velocity coupling between the momentum and the continuity equations.

The computational domain is the same as the present experimental setup. At the inlet, a uniform velocity profile ($u$=1, $v$=$w$=0) is imposed, while the convective boundary condition is used at the outlet. The no-slip boundary condition is prescribed at the surfaces of the tubes and the lateral surfaces. However, the periodic boundary condition is employed at the boundaries in the spanwise direction to reduce the time consumption. The validation test is also performed before the present simulations.

## 3. VELOCITY DISTRIBUTIONS

### 3.1 Laminar flow around the tube bundles

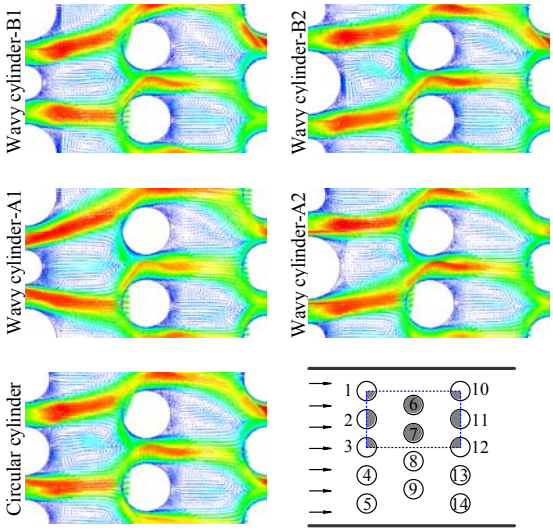


Figure 3: *Time average velocity vector distributions of wavy and circular tube bundles in the x-y planes at Re=100. (WY-A: $\lambda/D_m$=1.5, $a/D_m$=0.15; WY-B: $\lambda/D_m$=6, $a/D_m$=0.15)*

Figure 3 shows the time average velocity vector distributions of wavy and circular tube bundles in the *x-y* planes at *Re*=100. The Reynolds numbers are based on the oncoming flow and the mean diameter $D_m$ of the circular and wavy cylinders. For the wavy tube bundle cases, considering the out-of-phase arranged wavy tubes in the first row, two cross-section planes are plotted namely wavy cylinder-A1, A2 and B1, B2 respectively. In general, the velocities distributions at the positions of wavy tube gaps (WY-A) are higher than that of circular tubes, while the velocities of WY-B are slightly lower than that of circular tubes. The evidently different of velocity distribution of the first row tubes for WY-A and WY-B are due to the different separation angles of these two wavy cylinders with the wavelength ratios of $\lambda/D_m$=1.5 and 6. The separation angle at the nodal plane is larger than that at the saddle plane for the wavy cylinder with a smaller wavelength $\lambda/D_m$=1.5 (Lam and Lin 2008), while at the nodal plane, it is smaller than that at the saddle plane for the wavy cylinder with a larger wavelength $\lambda/D_m$=6 (Lam and Lin 2007). The large gaps velocity at the first row implied the drag force increasing for the second row tubes.

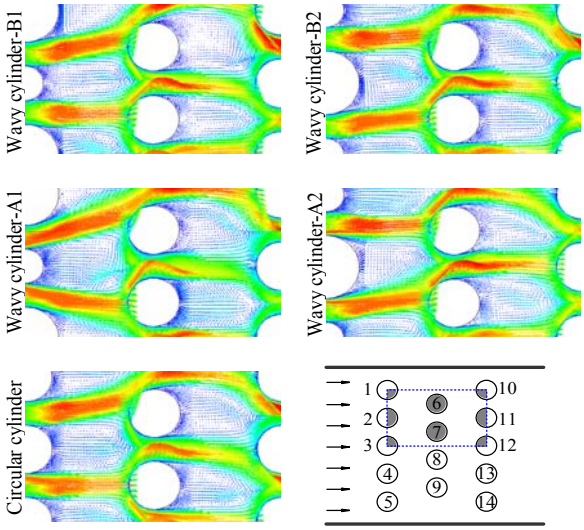


Figure 4: *Time average velocity vector distributions of wavy and circular tube bundles in the x-y planes at Re=200. (WY-A: $\lambda/D_m$=1.5, $a/D_m$=0.15; WY-B: $\lambda/D_m$=6, $a/D_m$=0.15)*

The same as those showed at *Re*=100, the time average velocity vector distributions in the *x-y* plane at *Re*=200 are plotted in figure 4. Similar velocity distributions are also obtained. The different of the first row gap velocity between the circular and wavy tubes are slightly reduced. It means the flow patterns and the velocity distribution have some relationships with the Reynolds numbers.

### 3.2 Turbulent flow around the tube bundles

The turbulent flow around tube bundles can be

found in many important engineering applications. By using the LES method and experimental measurements, some important results are obtained.

Figure 5 shows the time average velocity vector distributions of wavy and circular tube bundles in the *x-y* planes at *Re*=7500. Because of the effect of wavy tubes arranged at the first row (WY-B with the spanwise wavelength $\lambda/D_m$=6 and the wave amplitude $a/D_m$=0.15), the wake width of the second row tubes are larger than those with circular cylinder or wavy cylinder-A (WY-A, $\lambda/D_m$=1.5 and $a/D_m$=0.15) arranged in the first row. The wake patterns are well organized and the vortex shedding moved to further downstream positions compared with the tube bundle which arranged the circular tubes in first row and that of WY-A. It means the tube bundles' fluctuating forces will be weakened, especially for the second row tubes.

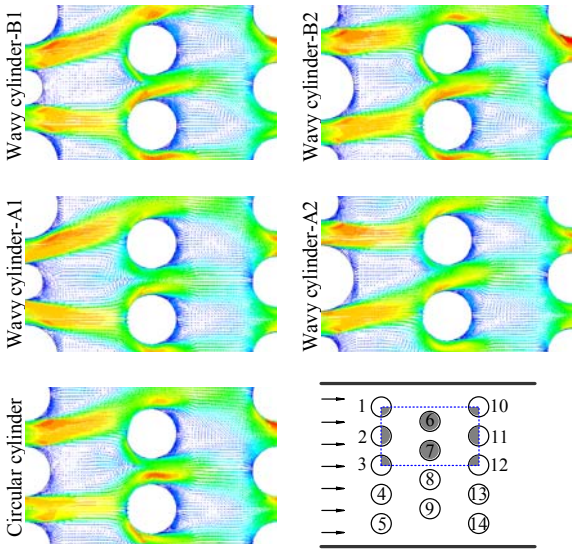


Figure 5: *Time average velocity vector distributions of wavy and circular tube bundles in the x-y planes at Re=7500. (WY-A: $\lambda/D_m$=1.5, $a/D_m$=0.15; WY-B: $\lambda/D_m$=6, $a/D_m$=0.15)*

The mean streamwise velocity distributions at the positions of $x/D_m$=1.5, 4 and 6 for wavy and circular tube bundles are plotted in figure 6 by using the LDA measurement, respectively. In general, the gap velocities behind the second row of tubes are evidently smaller than those behind the first and third row of tubes. However, no evident different can be found between those of circular and wavy tubes. It implies that the drag force may not be significantly reduced by using either circular cylinders or wavy cylinders in the first row of tubes. Such observations will be further discussed later.

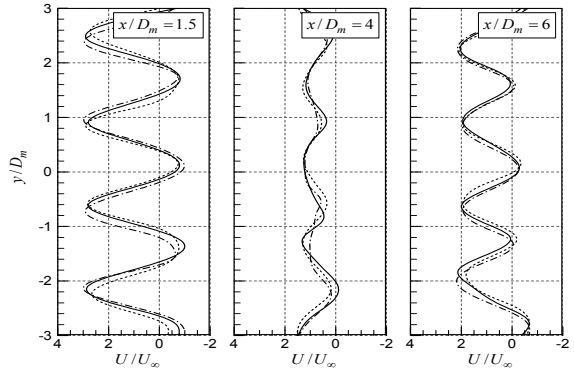


Figure 6: *LDA measurement of the streamwise velocity distributions at the positions of $x/D_m$=1.5, 4 and 6, respectively (Re=7500).The cross-section of the wavy tube bundles case is WY-A2 and WY-B2. The solid line ——— : case of CY; the dashed line ····· : case of WY-A and the dashdotted line -·-·-·- : case of WY-B.*

## 4. FORCE, FREQUENCY AND TURBULENT KINETIC ENERGY

### 4.1 Force characteristics

The mean drag coefficients and the root-mean-square fluctuating lift coefficients for each tube are obtained (see figure 7). The drag coefficient $C_D$ and lift coefficient $C_L$ in the present simulations are defined by

$$C_D = 2F_D / \rho U_\infty^2 D_m \lambda \quad (4)$$

$$C_L = 2F_L / \rho U_\infty^2 D_m \lambda \quad (5)$$

where $\rho$ is the fluid density, $U_\infty$ is the incoming flow, $F_D$ and $F_L$ are the total drag force and total lift force, respectively.

The mean drag coefficients for wavy tubes are not reduced compared with the circular tubes in the first row. It is same as those in the second and third rows. Lam et al. (2004b) reported that an elongation of the formation length for wavy cylinder will give rise to a higher back pressure in the rear side of a single cylinder, which is the most important contribution in producing a low drag force. It would be interesting to see whether the wavy cylinders will bring about the same effects on tube bundles. However, the present results show that this characteristic for drag force reduction is not generated for wavy tube bundles at such spacing ratio. However, some interesting results are obtained concerning the fluctuating lift coefficients. The present results showed the out-of-phase arranged wavy tubes (WY-B, $\lambda/D_m$=6 and $a/D_m$=0.15) give rise to a more stable flow pattern

with less fluctuation, especially for the effect on the second row of tubes. The fluctuating lift coefficients for the tube bundle (WY-B) are all less than those tube bundles (WY-A or CY).

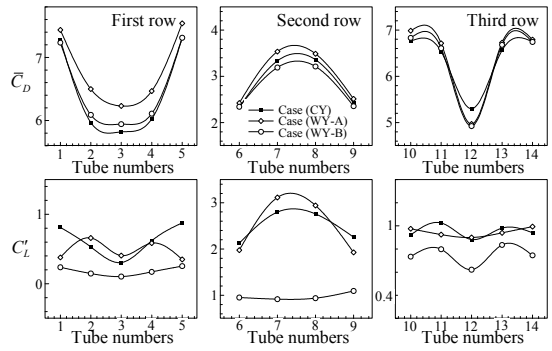


Figure 7: *Mean drag coefficients and fluctuating lift coefficients for each wavy and circular tube at Re=7500.*

## 4.2 Turbulent kinetic energy

Figure 8 shows the turbulent kinetic energy (TKE) in the *x-y* planes at *Re*=7500.

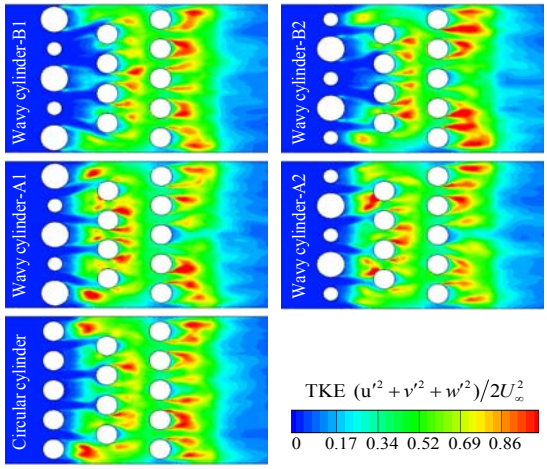


Figure 8: *Normalized turbulent kinetic energy (TKE) distributions for wavy and circular tube bundles at different cross sections in the x-y plane. (WY-A: λ/D$_m$=1.5, a/D$_m$=0.15; WY-B: λ/D$_m$=6, a/D$_m$=0.15)*

Compared with the circular tubes in the first row, the region of negligible kinetic energy is noticeably larger behind the wavy tubes (WY-B). All the TKE values for different planes of the tube bundle (WY-B) are smaller than that of the circular bundle. It suggests that this kind of wavy geometry can significantly reduce the TKE in the near wake. That implies the force of the collision exerting on the second tube row will be weakened and in turn, the suppression of the fluctuating lift. It also confirms that why the fluctuating lift coefficients of the second row tubes for tube bundle (WY-B) are smaller than those for tube bundles (CY and WY-A). Moreover, no significant different of the TKE between the tube bundle CY and WY-A were observed.

## 4.3 Frequency and vibration control

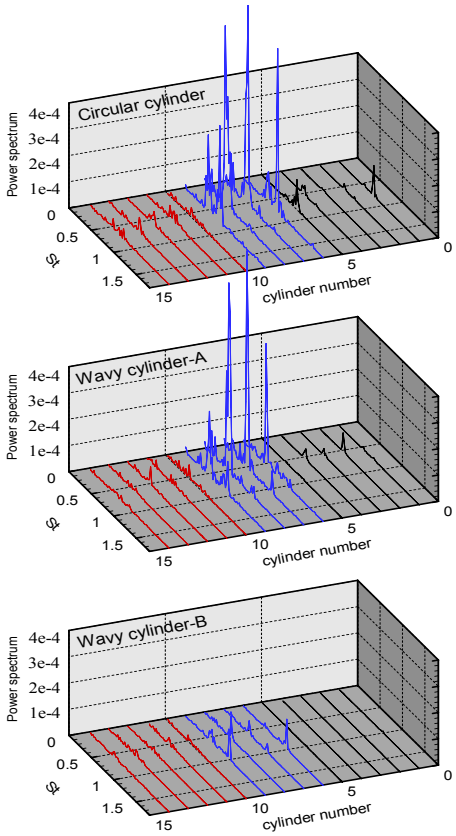


Figure 9: *Strouhal numbers of different wavy and circular tubes at Re=7500. (WY-A: λ/D$_m$=1.5, a/D$_m$=0.15; WY-B: λ/D$_m$=6, a/D$_m$=0.15)*

The Strouhal number is the non-dimensional frequency $f_S$ of vortex shedding, and is expressed as

$$St = f_S D_m / U_\infty \qquad (6)$$

In the present study, the frequency of vortex shedding is obtained by Fast Fourier Transform (FFT) of the lift force coefficient fluctuating time history. The values of Strouhal number for each circular or wavy tube are plotted in figure 9. The same as the results of the TKE, by arranged the wavy tubes (WY-B) in the first row, the vortex shedding frequency are evidently suppressed considering the power spectrum. It also confirms that a heat exchanger tube bundle composed of circular and some typical wavy cylinder may be used to control the flow-induced vibration.

## 5. CONCLUSION

Flow around heat exchanger tube bundles composed of circular and wavy cylinders are investigated numerically and experimentally. Both the laminar and turbulent flows are examined. Two types of tube bundles with the first row of tubes replaced by different wavy cylinders are compared with that of purely circular cylinders. For the turbulent flow, in general, the drag force is not evidently reduced by using such compositions. However, the lift fluctuating is evidently weakened for the wavy tubes with $\lambda/D_m$= 6 and $a/D_m$=0.15 in an out-of-phase arrangement. Because of the effect of this kind of wavy tubes arranged at the first row, the turbulent kinetic energy behind the first row tubes are reduced and the wake patterns of the second row tubes are well organized compared with the tube bundle with circular tubes in first row. That implies the force of the collision exerting on the second tube row will be weakened. It also means the bodies' fluctuating force will be weakened. It is hopeful that these kinds of wavy tube arrangements can be used to control of the cross-flow induced vibration of a large numbers of tube bundles in heat exchanger.

## 6. ACKNOWLEDGEMENTS

The authors wish to thank the Research Grants Council of the Hong Kong Special Administrative Region, China, for its support through Grant No. PolyU 5188/05E.

## 7. REFERENCES

Barsamina, H.R., Hassan, Y.A., 1997, Large eddy simulation of turbulent cross flow in tube bundles. *Nuclear Engineering and Design*, **172**: 103-122.

Horvat A. et al, 2006, Comparison of heat transfer conditions in tube bundle cross-flow for different tube shapes. *International Journal of Heat and Mass Transfer*, **49**: 1027-1038.

Kevlahan, N.K.-R., Wadsley, J., 2005, Suppression of three-dimensional flow instabilities in tube bundles. *Journal of Fluids and Structures*, **20**: 611-620.

Lam, K. et al, 2004a, Experimental investigation of the mean and fluctuating forces of wavy (varicose) cylinders in a cross-flow. *Journal of Fluids and Structures*, **19**: 321-334.

Lam, K. et al, 2004b, Three-dimensional nature of vortices in the near wake of a wavy cylinder. *Journal of Fluids and Structures*, **19**: 815-833.

Lam, K., Lin, Y.F., 2007, Drag force control of flow over wavy cylinders at low Reynolds number. *Journal of Mechanical Science and Technology*, **21**: 1331-1337.

Lam, K. et al, 2007, Flow characteristics around a row of circular and wavy cylinders. *Journal of Mechanical Science and Technology*, **21**: 1910-1917.

Lam, K., Lin, Y.F., 2008, Large eddy simulation of flow around wavy cylinders at a subcritical Reynolds number. *International Journal of Heat and Fluid Flow*, (accepted)

Paul, S.S. et al, 2007, Experimental study of turbulent cross-flow in a staggered tube bundle using particle image velocimetry. *International Journal of Heat and Fluid Flow*, **28**: 441-453.

Price, S.J. et al, 1995, Flow visualization of the interstitial cross-flow through parallel triangular and rotated square arrays of cylinders. *Journal of Sound and Vibration*, **181**: 85-98.

Rottmann, M., Popp, K., 2003, Influence of upstream turbulence on the fluidelastic instability of a parallel triangular tube bundle. *Journal of Fluids and Structures*, **18**: 595-612.

Schneider, K., Farge, M., 2005, Numerical simulation of the transient flow behaviour in tube bundles using a volume penalization method. *Journal of Fluids and Structures*, **20**: 555-566.